VERY LARGE ARRAY DETECTION OF RADIO RECOMBINATION LINES FROM THE RADIO NUCLEUS OF NGC 253: IONIZATION BY A WEAK ACTIVE GALACTIC NUCLEUS, AN OBSCURED SUPER STAR CLUSTER, OR A COMPACT SUPERNOVA REMNANT?

Niruj R. Mohan

Raman Research Institute, C. V. Raman Avenue, Sadashivanagar Post Office, Bangalore 560-080, India;
and Joint Astronomy Program, Department of Physics, Indian Institute of Science, Bangalore 560-012, India; niruj@rri.res.in

K. R. Anantharamaiah[1]

Raman Research Institute, C. V. Raman Avenue, Sadashivanagar Post Office, Bangalore 560-080, India

and

W. M. Goss

National Radio Astronomy Observatory, P.O. Box O, Socorro, NM 87801; mgoss@aoc.nrao.edu

ABSTRACT

We have imaged the H92α and H75α radio recombination line (RRL) emissions from the starburst galaxy NGC 253 with a resolution of $\sim$4 pc. The peak of the RRL emission at both frequencies coincides with the unresolved radio nucleus. Both lines observed toward the nucleus are extremely wide, with FWHMs of $\sim$200 km s^{-1}. Modeling the RRL and radio continuum data for the radio nucleus shows that the lines arise in gas whose density is $\sim$10^4 cm^{-3} and mass is a few thousand $M_\odot$, which requires an ionizing flux of $(6–20) \times 10^{51}$ photons s^{-1}. We consider a supernova remnant (SNR) expanding in a dense medium, a star cluster, and also an active galactic nucleus (AGN) as potential ionizing sources. Based on dynamical arguments, we rule out an SNR as a viable ionizing source. A star cluster model is considered, and the dynamics of the ionized gas in a stellar-wind driven structure are investigated. Such a model is only consistent with the properties of the ionized gas for a cluster younger than $\sim$10^5 yr. The existence of such a young cluster at the nucleus seems improbable. The third model assumes the ionizing source to be an AGN at the nucleus. In this model, it is shown that the observed X-ray flux is too weak to account for the required ionizing photon flux. However, the ionization requirement can be explained if the accretion disk is assumed to have a big blue bump in its spectrum. Hence, we favor an AGN at the nucleus as the source responsible for ionizing the observed RRLs. A hybrid model consisting of an inner advection-dominated accretion flow disk and an outer thin disk is suggested, which could explain the radio, UV, and X-ray luminosities of the nucleus.

Subject headings: galaxies: individual (NGC 253) — galaxies: ISM — galaxies: nuclei —
galaxies: starburst — radio lines: galaxies

1. INTRODUCTION

NGC 253 is a nearby ($D = 2.5$ Mpc) spiral galaxy with the central $\sim$100 pc hosting a vigorous starburst. The ionized gas in this region, studied by its emission in the radio, infrared (IR), and optical, consists of both compact and diffuse components and is distributed along a highly inclined ring. Turner & Ho (1985) discovered a string of compact sources at 15 GHz, which were studied in detail by Antonucci & Ulvestad (1988) and Ulvestad & Antonucci (1997). A number of IR hotspots have also been imaged in this region (Forbes, Ward, & Depoy 1991; Forbes et al. 1993; Piña et al. 1992; Keto et al. 1993; Sams et al. 1994). Kalas & Wynn-Williams (1994) and Sams et al. (1994) showed that most of these hotspots are regions of low dust extinction and are not coincident with the radio sources. Optical imaging by Watson et al. (1996) revealed the presence of four star clusters, which were identified with individual IR knots (see also Forbes et al. 2000). The radio and the IR–optical sources seem to trace different populations of objects, presumably supernova remnants (SNRs) and H II regions, respectively. Radio recombination lines (RRLs) have been observed from this galaxy in the centimeter (Seaquist & Bell 1977; Mebold et al. 1980; Anantharamaiah & Goss 1996) and millimeter (Puxley et al. 1997) wave bands with a resolution of a few arcseconds ($1'' = 12$ pc) or larger. Since IR and radio continuum images are now available with subarcsecond resolution, the identification of the exact sources of RRL emission using high-resolution imaging becomes relevant.

The peak of the IR emission is offset by about 3$\overset{''}{.}$5 southwest from the peak of the radio continuum emission (the radio nucleus). There is no associated radio emission toward the IR peak and weak IR emission is observed near the radio nucleus. Keto et al. (1999) have shown that the IR peak hosts a super star cluster (SSC), and they have also suggested that the radio nucleus is probably an active galactic nucleus (AGN). Turner & Ho (1985), based on their high-resolution Very Large Array (VLA) image of the 15 GHz continuum emission, discovered that the radio nucleus is an unresolved source with high brightness temperature and suggested that the nucleus could harbor an AGN. Multiband tracers of ionized gas ([Ne II]: Böker, Krabbe, & Storey 1998; Keto et al. 1999; Brγ: Forbes et al. 1993; optical continuum and line emission: Engelbracht et al. 1998; Watson et al. 1996; Forbes et al. 2000) show that the maximum emission at these wave bands coincides with the

[1] Deceased 2001 October 29.

position of the IR peak. It is therefore surprising that the centimeter-wave RRL emission imaged by Ananthara-maiah & Goss (1996) with a resolution of $1\rlap{.}''8 \times 1''$ shows that the recombination line emission peaks at the radio nucleus, with much weaker emission near the IR peak. In order to further investigate the characteristics of this emission, we have carried out subarcsecond observations of the RRL emission from NGC 253 at 8.3 and 15 GHz using the VLA. These observations will help identify the compact continuum sources from which the RRLs observed at low resolutions originate. In addition, since the peak of the line emission is probably coincident with the radio nucleus, the physical properties of the ionized gas in this region, and hence the nature of the nuclear source, can be derived by modeling the RRL emission.

2. OBSERVATIONS AND RESULTS

The 8.3 GHz H92α and the 15 GHz H75α recombination lines from NGC 253 were observed using the VLA of the National Radio Astronomy Observatory in the A configuration. This observing mode yields the required parsec-scale resolution with the best sensitivity possible. The data analysis was done using standard procedures available in the software package AIPS. The data sets at 8.3 GHz, acquired over three periods, were concatenated for further processing. Of the two data sets available at 15 GHz, only one was used, as the other suffered from bandpass problems. Continuum images were made at both frequencies and are consistent with the images published by Ulvestad & Antonucci (1997). The channel visibilities, after Hanning smoothing off-line to reduce the effects of Gibbs ringing, were used to construct line data cubes. The continuum and line images at both frequencies were convolved to a common resolution of $0\rlap{.}''35 \times 0\rlap{.}''22$ at a P.A. of $-10°$. The shortest baselines in the data sets are mentioned in Table 1. The largest well-sampled angular scale in the images is estimated to be $\sim 7\rlap{.}''5$ at 8.3 GHz and $\sim 3\rlap{.}''0$ at 15 GHz.

The continuum emission at 8.3 and 15 GHz from the central $3''$ region is shown in Figure 1. Also shown in the figure

are overlays of the integrated line emission. The H92α and H75α spectra toward the peak of the line emission are shown in Figure 2. Further observational details and image parameters are listed in Table 1. The peak of the continuum emission corresponds to the radio nucleus and is associated with the source 5.79−39.0 in the compact source catalog of Ulvestad & Antonucci (1997). Although the central $3''$ region contains multiple sources, the nucleus is separable from the surrounding emission with our resolution of $0\rlap{.}''3$. The peaks of both the H92α and H75α line emission coincide with the unresolved radio nucleus, with much weaker emission near the IR peak. Extended H92α line emission is detected over a $3''$ region. Since the 8.3 GHz data sets were imaged with less weighting given to short spacing visibilities in order to have similar resolution as that of the 15 GHz data, this diffuse emission is not detectable in Figure 1. In this paper, we only discuss the line emission detected against the unresolved radio nucleus. The discussion of the extended line emission as well as the emission toward other compact sources in the field will follow in a later paper.

3. MODELING THE RRL EMISSION

The properties of the ionized gas at the nucleus were modeled using the observed continuum and recombination lines. These observational constraints correspond to an area of ~ 4 pc (one synthesized beam), and the values are listed in Table 1. The line-emitting gas was assumed to be photoionized, and the atomic level populations were derived assuming that the gas is not in local thermodynamic equilibrium (non-LTE). The ionized gas was modeled as a single spherical H II region, as a collection of H II regions, and also as a rectangular slab. Since the results are similar in all three cases, we only discuss the spherical H II region model. The free parameters of the model are electron density n_e, diameter l of the H II region, and electron temperature T_e; the range of parameter space is indicated in Table 2. The density was assumed to be uniform inside the H II region. The relative locations of both the line-emitting thermal gas and the nonthermal continuum source along the line of sight within

TABLE 1
VLA Observational Log and Image Parameters

Parameter	8.3 GHz Data	15 GHz Data
Date of observation	1999 Jul 9, Jul 12, and Oct 9	1999 Jun 26
ν_{rest} of RRL (GHz)..	8309.4 (H92α)	15281.5 (H75α)
Bandwidth (MHz), channels/IF...........................	24.2, 31	46.9, 15
Spectral resolution[a] (km s^{-1})	56.4	122.6
Shortest baseline (kλ)..	7	12
Beam (natural weights)	$0\rlap{.}''5 \times 0\rlap{.}''28$	$0\rlap{.}''31 \times 0\rlap{.}''14$
Phase calibrator	0116−219	0118−272
Bandpass calibrator	2251+158	2251+158
Peak continuum flux density[b] (mJy)	40	37
Peak line flux density (mJy)	0.92 ± 0.02	1.72 ± 0.02
Noise in the continuum image (1 σ) (mJy)..............	0.04	0.13
Line strength[c] ($\times 10^{-23}$ W m^{-2})............................	6 ± 1	23 ± 2
FWHM of line[d] (km s^{-1})	225 ± 15	197 ± 26
Noise per channel (mJy)..	0.14	0.35

[a] The spectral resolution after off-line Hanning smoothing.
[b] Evaluated by simultaneously fitting a Gaussian, a zero level, and a slope.
[c] Corresponding to the spectrum against the unresolved radio nucleus.
[d] The FWHM after deconvolving the effects of Hanning smoothing and finite spectral resolution.
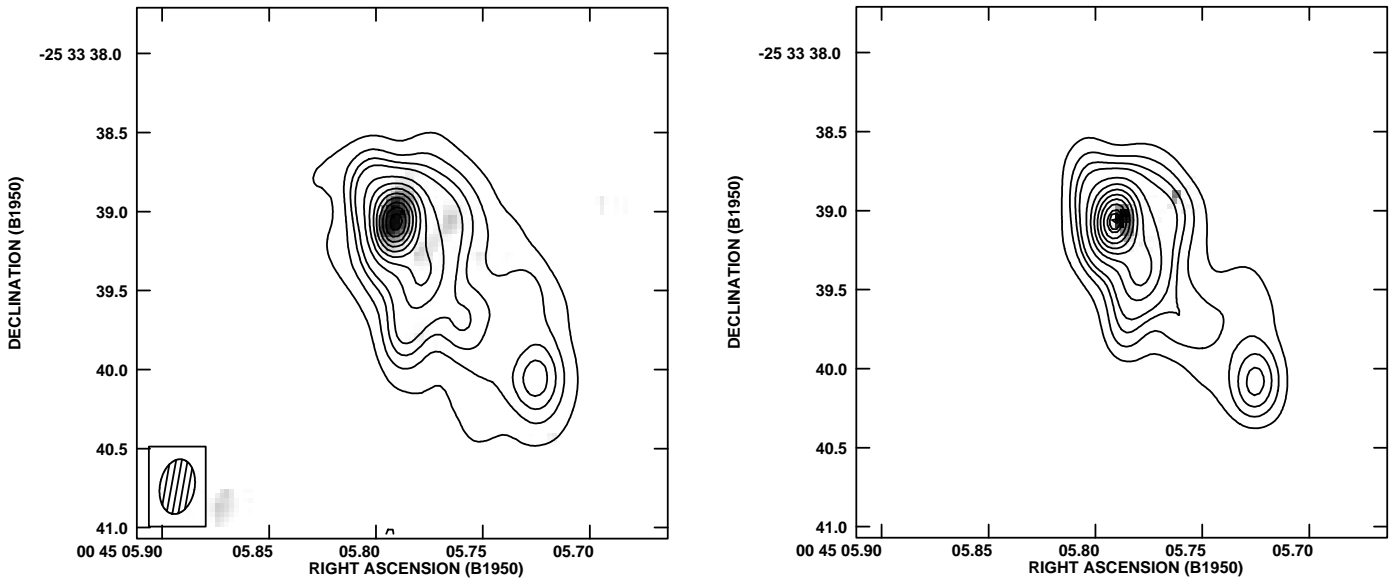
Fig. 1.—Radio continuum emission at 8.3 (*left*) and 15 (*right*) GHz of the central 36 pc of NGC 253, plotted as contours. The contour levels in mJy are 4, 6, 8, and 10 and then higher in steps of 5 mJy. The line emission integrated over the velocity range 100–400 km s^{-1} for the H92α and H75α RRLs is superposed in gray scale. The beam size for both the images is 0$\farcs$35 × 0$\farcs$22 at a P.A. of −10° and is shown at the bottom left corner of the left panel.

the synthesized beam are unknown. Hence, the fraction of the nonthermal continuum radiation that is behind the thermal gas (and is responsible for stimulated line emission due to background radiation) is varied from zero to the total observed flux density in the models. For every combination of n_e, l, and T_e, the continuum and line emission strengths were then calculated. Of these combinations, those models that reproduce the observed line strengths at both frequencies and also predict continuum flux densities consistent with the observed values were accepted as valid solutions. The spectral index of the unabsorbed continuum (which includes the nonthermal part as well the thermal part that

does not contribute to the observed line emission) was also calculated and was constrained to not be steeper than −1.0. The details of the modeling technique are discussed in detail by Anantharamaiah et al. (1993).

The ranges of values for various solutions are indicated in Table 2. The results do not depend sensitively on the assumed value of the electron temperature within the range explored. Typical parameters of the line-emitting gas are listed in Table 3 for specific models. The allowed models described in Tables 1 and 2 assume that the unabsorbed continuum fills the synthesized beam. No solutions are obtained if the gas is assumed to be in LTE; the linear size of
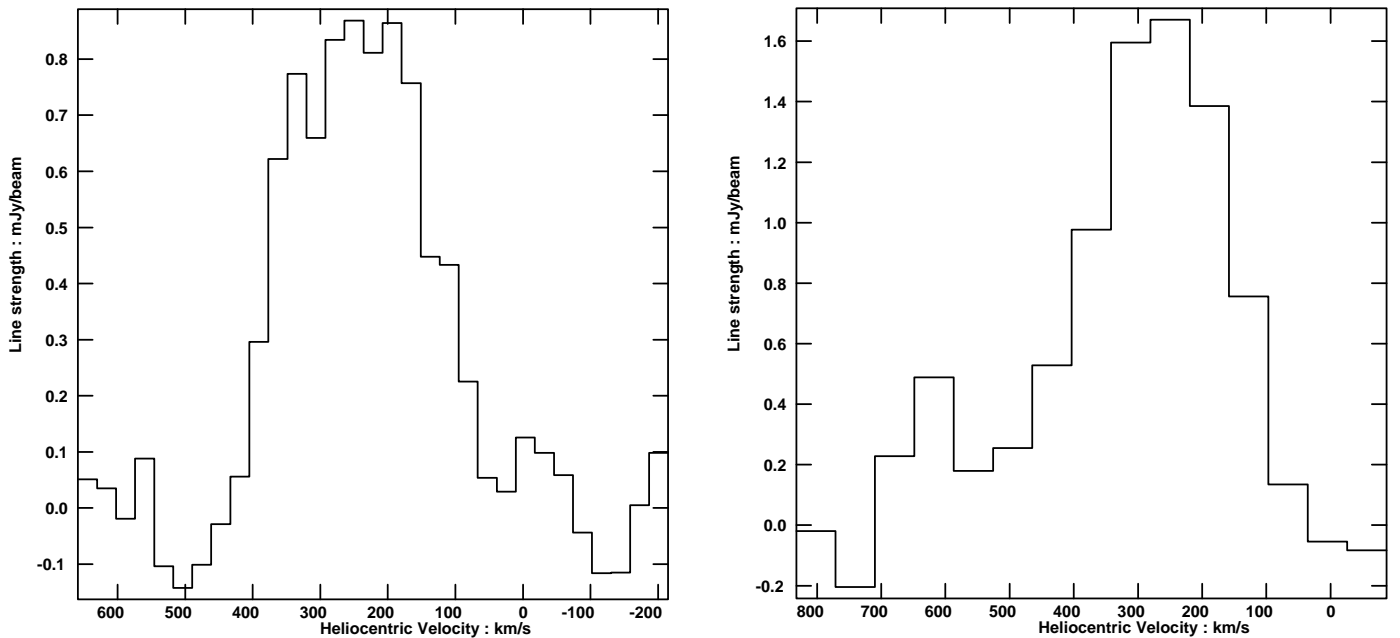

Fig. 2.—Hanning-smoothed spectra of H92α RRL at 8.3 GHz (*left*) and H75α RRL at 15 GHz (*right*) against the radio nucleus, for a resolution element of 0$\farcs$35 × 0$\farcs$22. The velocity resolution is 56.4 and 122.6 km s^{-1} for the H92α and H75α spectra, respectively.

Parameter	Range
Explored Input Parameter Space	
Electron temperature (T_e: K)	2500–12,500
Local electron density (n_e: cm^{-3})	10^{-2}–10^6
Diameter (l: pc)	0.01–5.0
Model Solutions for T_e = 5000–12,500 K	
n_e (cm^{-3})	6000–17,000
l (pc)	2–5.0
N_{Lyc} (s^{-1})	$(6-20) \times 10^{51}$
$M_{\mathrm{H\,II}}$ ($M_\odot$)	1000–7000
Stimulated emission (at 15 GHz) (%)	10–60
Thermal continuum fraction (at 15 GHz)	0.15–0.7

the region is too small and the background nonthermal radiation is too weak to produce a detectable RRL. Hence, line enhancement due to non-LTE processes is essential to explain the observed line strength. Only a narrow range of densities (6×10^3–1.7×10^4 cm^{-3}) is allowed, and the ionizing photon rate ranges from 6×10^{51} to 20×10^{51} photons s^{-1}. A power-law multidensity model was also considered (see model IV of Mohan, Anantharamaiah, & Goss 2001 for details). In this model, gas at densities that differ considerably from the values derived in this section do not contribute appreciably to the observed RRL emission (see Mohan et al. 2001). Hence, the constant-density approximation used in the models mentioned above is justified. For $n_e < 6 \times 10^3$ cm^{-3}, the computed line emissions inside a $\sim$4 pc region fall short of the observed values. For $n_e > 1.7 \times 10^4$ cm^{-3}, the model predictions do not agree with the observed H92α/H75α line ratio. The observations can be explained without invoking stimulated emission due to a background continuum radiation, i.e., the line emission can be explained solely by spontaneous emission by ionized gas, which includes stimulated emission by its own thermal continuum. For a given emission measure, inclusion of any externally stimulated emission enhances the recombination line strength compared to a case in which no background radiation is invoked. Hence, the mass of ionized gas needed and the required ionizing photon flux are both less by up to a factor of 2–3 for models incorporating nonthermal

continuum radiation. If the unabsorbed continuum is assumed to be a distributed uniform background, then the externally stimulated emission can account for up to 60%–70% of the total H75α line strength.

If these models are computed for either the H92α or the H75α line alone, the range of allowed densities obtained is larger. Including only the H92α line changes the lower limit to the allowed density to 2000 cm^{-3}, whereas densities as high as 10^5 cm^{-3} are allowed for models that incorporate only the H75α line. Thus, including both RRLs constrains the possible density to a much narrower range, assuming that all the observed line emission at both frequencies arises in the same region of ionized gas. Our models, therefore, show that the observed H75α and H92α lines arise in gas with a mass of a few thousand $M_\odot$ and a density of $\sim 10^4$ cm^{-3} and require an ionizing photon flux of $\geq 6 \times 10^{51}$ s^{-1}. The relative faintness of RRLs from near the IR peak and the absence of a strong radio counterpart to the IR peak, which is a massive SSC, do not necessarily imply that there is less gas at the latter position; the gas could be of lower density instead.

4. THE IONIZING SOURCE

The RRL detection from the unresolved radio nucleus is from a sufficiently small linear size that the interpretation is not complicated by the unknown beam filling factors of the gas. The derived ionizing photon flux inside a $\sim 0\farcs3$ (4 pc) region can be compared with the values computed from other tracers of ionized gas. Using photoionization models, this value corresponds to an Hα flux of 1.2×10^{-14} W m^{-2}. Forbes et al. (2000) list the Hα fluxes of compact optical sources measured inside a $0\farcs4$ aperture. Since the strength of the line emission at the position of the radio nucleus is weak (Watson et al. 1996; D. A. Forbes 2001, private communication), we can assume that the Hα flux from this area is less than that of the weakest source listed in their table. Then, the extinction derived using the Hα estimated from RRL modeling is $A_V > 14$ mag, consistent with the $A_V = 24 \pm 6$ mag derived by Sams et al. (1994) toward the radio nucleus. Measurements of other IR emission lines from ionized gas correspond to much larger apertures, and since the region surrounding the radio nucleus does contain significant amounts of ionized gas, a direct comparison is difficult. Nevertheless, if we assume a uniform extinction of 25 mag in the central region, then the extinction-corrected

PARAMETER	n_e= 7000 cm^{-3}			n_e = 17,000 cm^{-3}		
	A[a]	B	C	A	B	C
Diameter l (pc)	3.1	4.0	3.5	2.1	2.3	2.1
N_{Lyc} ($\times 10^{52}$ s^{-1})	0.8	1.6	1.0	1.4	1.9	1.4
$S_{\mathrm{th}}/S_{\mathrm{total}}$ at 15 GHz	0.3	0.6	0.4	0.4	0.5	0.4
Stimulated emission[b] (%)	55	0	...	22	0	...
Spectral index[c] α ($S_\nu \propto \nu^{-\alpha}$)	0.45	0.5	0.45	0.7	0.75	0.7
$M_{\mathrm{H\,II}}$ ($M_\odot$)	2800	6000	3700	2100	2800	2200

[a] A, B, and C refer to models in which the unabsorbed continuum radiation is assumed to be behind, in front of, and mixed with the ionized gas, respectively.

[b] The fraction of H75α line emission due to stimulated emission by the background radiation.

[c] Average spectral index of the unabsorbed continuum radiation, excluding the thermal contribution of the ionized gas.

Brα flux from the central 6″ (from the data of Beck & Beckwith 1984) is a factor of 10 higher than the predictions of our model for the $\sim$0″.3 region of the nucleus. Forbes et al. (1993) measured the Brγ emission inside a 2″ aperture centered around the radio nucleus (referred to as spot A). The Brγ flux measured by them is a factor of 2 higher than the value predicted by our models, this excess being possibly due to their larger aperture.

Since the region of interest is highly obscured, the source of the photoionization remains uncertain. We consider three possible candidates: (1) an SNR expanding in a dense medium, (2) a stellar cluster, and (3) an AGN. Each of these are now examined in detail to investigate which of these can explain the observed properties of the nuclear region. The imposed constraints are the derived properties of the ionized gas, such as density, size, ionizing flux, and line width, and also the radio, UV (derived from ionization), and X-ray luminosities of the nucleus. The 2–10 keV X-ray luminosity (L_{2-10}) of the X-ray source coincident with the radio nucleus is 7×10^{38} ergs s^{-1} (unresolved for $E > 2$ keV; Pietsch et al. 2001, using the *XMM-Newton*).

5. A COMPACT SUPERNOVA REMNANT AS AN IONIZING SOURCE

Chevalier & Fransson (2001) invoked an SNR expanding into a dense ambient medium to explain some of the compact radio sources in the starburst galaxy M82 and in Arp 220 as well, and we now consider such a model to explain the nucleus of NGC 253. The high ambient density slows down the expansion to a few 100 km s^{-1}, confines the remnant to a smaller size, and causes it to quickly enter the radiative or snowplow phase. These factors could explain the spatial extent (≤ 4 pc) and the line width (attributed to the expansion of the remnant) of the ionized gas. In the snowplow phase, the swept-up gas cools and forms a thin shell and can be ionized by the X-ray photons from the hot gas inside the remnant, giving rise to the observed RRLs. We have calculated the dynamics and radiation of such an SNR in an attempt to explain the RRL observations. In our model, the input parameters are the initial energy of the explosion E_0, the ambient density n_0, and the age of the compact SNR. Following the work of Draine & Woods (1991), we calculate the velocity and radius of the shock front and also the ionization rate and the density of ionized gas in the shell as a function of time, E_0, and n_0. The time-dependent value of L_{2-10} is also computed for both the Sedov phase (using the similarity solutions; Newman 1977) and for the radiative phase. The observed values (listed in Tables 1 and 2) are compared with these calculated values for the radiative phase of the SNR (when an expanding recombining gas is produced). We find that the models cannot simultaneously satisfy all of these constraints for any combination of input parameters. Hence, the properties of the nucleus cannot be explained by an SNR expanding in a dense medium.

6. A STAR CLUSTER AS AN IONIZING SOURCE

In this section, we assume that the nucleus hosts a stellar cluster and derive its properties. The number of O stars necessary to produce more than 6×10^{51} photons s^{-1} is more than 450, and the total mass of the cluster is more than 8.5×10^4 $M_\odot$ (computed assuming a Salpeter initial mass function [IMF] with a mass range between 1 and 80 $M_\odot$ and

using the tables in Vacca, Garmany, & Shull 1996). Since the region modeled is $\sim$4 pc in extent, the resultant total stellar mass and the lower limit to the stellar surface density imply that the ionizing source must be an SSC (Meurer et al. 1995). The RRLs are assumed to arise in the H II region around this SSC (similar to "supernebulae" discovered in the centers of other galaxies; Kobulnicky & Johnson 1999; Neff & Ulvestad 2000; Tarchi et al. 2000; Turner, Beck, & Ho 2000; Mohan et al. 2001). The detection of wide lines with FWHM of $\sim$200 km s^{-1} from within a $\sim$4 pc region is a constraint on the dynamics of the nebula, which we investigate below. It should be noted that the dynamical age of the gas ($\sim$radius/velocity) is $\sim 10^4$ yr, and the sound crossing time is $\sim 10^5$ yr.

6.1. Gas Dynamics of the Supernebula

Although an H II region ionized by a central cluster will expand outward, its expansion velocity can never exceed the speed of sound in the ionized medium (Spitzer 1968) and hence cannot account for the wide lines observed. In addition, champagne flows in H II regions cannot produce velocities larger than $\sim$50 km s^{-1} (Yorke, Tenorio-Tagle, & Bodenheimer 1984). Although supersonic velocities are known in extragalactic H II regions, their line widths are only $\sim$30–100 km s^{-1}, and the H II regions are also much larger in size (for, e.g., Muñoz-Tuñón, Tenorio-Tagle, & Casteñada 1996). The only plausible way to explain the observed velocity width is by invoking a stellar-wind–driven H II region expanding at $\sim$100 km s^{-1}. The expansion velocity of a wind-driven shell scales as $L_{\mathrm{mech}}^{1/5}$, where L_{mech} is the mechanical luminosity of the wind, and hence an expansion velocity of 100 km s^{-1} for a cluster whose L_{mech} is $\sim 10^3$ times that of an O star is easily obtainable. The dynamical age of a wind-driven shell is $\sim 0.55 R_{\mathrm{shell}}/V_{\mathrm{shell}}$ (McCray 1983), i.e., $\sim 10^4$ yr.

The model considered here is that of a uniform-density nebula whose dynamics are determined by the ionizing photons and the stellar wind of a central SSC. In the wind-driven phase of expansion, the nebula quickly enters the snowplow phase ($\leq 10^3$ yr), wherein it can be either in the energy-conserving or in the momentum-conserving phase. The swept-up matter forms a thin shell that is assumed to trap all the ionizing photons. The input parameters are the star formation history of the cluster, the constant ambient density (n_0), and the age of the cluster (assumed to be the same as the nebula), and the range of parameter space explored is summarized in Table 4. The time-dependent values of N_{Lyc} and L_{mech} were derived from simulations using the code STARBURST 99[2] (Leitherer et al. 1999). This simulation was carried out for solar metallicity and a Salpeter IMF with an upper mass cutoff of 100 $M_\odot$. These values were obtained for both a continuous and an instantaneous star formation history for a particular value of star formation rate (SFR) and subsequently scaled linearly for other values of SFR. For a given combination of input parameters, the radius and velocity of the shock front (almost the same as that of the ionized gas), mass of ionized gas, ionization rate, and the gas density were computed. These calculations were carried out using the expressions in Shull (1980) for the appropriate phase of the nebula. The derived values

---

[2] See http://www.stsci.edu/science/starburst99/.

TABLE 4
DYNAMICAL MODELING DETAILS

Parameter	Explored Range	Solutions Obtained
Parameter Space for Model Inputs		
Ambient density (n_0: cm^{-3})......................	10^{-3}–10^6	200–400
Age of cluster (yr)...................................	10^4–10^8	$(2$–$3.5) \times 10^4$
SFR ($M_\odot$ yr^{-1})..	0.1–100.0	2.5–6
Parameter Space for Observational Constraints		
Radius of shell (R_s: pc)	0.2–4.0	3.5–4.0
Velocity of shell (V_s: km s^{-1})	80–120	85–115
Mass of ionized gas ($M_\odot$)	1250–5000	1250–2400
$N_{\rm Lyc}$ (photons s^{-1}).................................	$(6$–$24) \times 10^{51}$	$(6$–$10) \times 10^{51}$
Density of ionized gas (n_e: cm^{-3})	$(4$–$25) \times 10^3$	$(18$–$25) \times 10^3$

were compared with the values derived from the RRL modeling, listed in Table 4. Acceptable solutions were identified that were consistent with the imposed constraints. Table 4 summarizes the allowed parameters.

Gas dynamics narrowly constrain the properties of the possible supernebula. The derived solutions correspond to wind-driven shells in the energy-conserving phase. The allowed age of the nebula (and hence the cluster) is $\sim 2.5 \times 10^4$ yr, corresponding to a diameter of 7–8 pc; no solutions for smaller sizes were found. These values are a strong constraint on the hypothesized SSC. However, the reliability of these values depends on the accuracy of the STARBURST 99 code for young clusters, as discussed in § 8.1.

7. A WEAK AGN AS AN IONIZING SOURCE

Turner & Ho (1985) discovered that the nucleus is unresolved in the radio continuum and has a high brightness temperature and hence suggested a possible AGN at the nucleus. Ulvestad & Antonucci (1997) also arrived at the same conclusion based on their higher resolution images. The derived size is less than 0″.05, and the lower limit to the brightness temperature is between 22,000 and 90,000 K. If an AGN does exist at the nucleus, then its UV continuum can be invoked to ionize the RRL-emitting gas. The expected UV luminosity can be estimated using the observed radio continuum and X-ray luminosities. Based on the upper limit to the size of the ionized gas and the observed line width, the dynamical mass at the center ($\sim \sigma^2 r / G$) is constrained to be less than $3 \times 10^6 M_\odot$.

Powerful AGNs are powered by a geometrically thin standard accretion disk whose blackbody emission peaks in the UV, called the big blue bump (BBB; Koratkar & Blaes 1999), which can provide the required ionization. Falcke, Malkan, & Biermann (1995) showed that this BBB luminosity is correlated with the core radio emission (νL_ν at 2 cm) for a sample of quasars. Extrapolating their relation for radio-weak quasars for the 2 cm luminosity of NGC 253, which is about 100 times less than their sample, the BBB luminosity for the nucleus is estimated to be $\sim 10^{42}$ ergs s^{-1}. This UV luminosity corresponds to an ionizing photon flux of $\sim 2 \times 10^{52}$ s^{-1}, consistent with the value derived from the observed RRLs. Based on the derived UV luminosity, the value of L_{2-10} was calculated for a range of input parameters (Frank, King, & Raine 1985). It was found that the thin-

disk model underpredicts L_{2-10} and is only consistent with observations for super-Eddington accretion rates.

However, given the low radiative efficiency of the nucleus (the accretion rate is estimated to be less than 0.01 times the Eddington rate), the AGN could be powered by an ADAF disk (Narayan, Mahadevan, & Quataert 1998). ADAF models predict the absence of a BBB. The 2 cm radio luminosity of the nucleus of NGC 253 implies that the AGN is of low luminosity (LLAGN; Nagar et al. 2000), and these LLAGNs have been shown not to exhibit a BBB in their UV emission (Ho 1999). Hence, we now try to explain the ionization from the X-ray luminosity instead. Pietsch et al. (2001) modeled the emission from the nuclear X-ray source as bremsstrahlung radiation from a three-temperature plasma. For simplicity, we assume that the UV up to X-ray emission is bremsstrahlung radiation from plasma at a single temperature $T_{\rm X}$. The UV portion of the emission is constrained to produce an ionizing photon flux greater than that needed to explain the RRLs, and the 2–10 keV portion is normalized to the observed value. The required ionization is only found to be consistent with the observed X-ray flux for $T_{\rm X} < 0.2$ keV. Since it is unlikely that most of the 2–10 keV emission arises in the exponentially decaying part of the thermal emission at 0.2 keV, this result is interpreted to imply that the X-ray emission is too weak to explain the required ionization.

8. DISCUSSION

8.1. *The Star Cluster Model*

Given the uncertainty of stellar tracks, $N_{\rm Lyc}$ and $L_{\rm mech}$ predicted by the STARBURST 99 code are not accurate to more than a factor of a few for $t < 5 \times 10^5$ yr (C. Leitherer 2001, private communication). The radius of the shock front is $R_s \sim (\int L_{\rm mech}\, dt)^{1/5}$ in the energy-conserving phase. Since $L_{\rm mech}$ is a monotonically increasing function of time (up to 5×10^6 yr for a continuous SFR), the dynamics of the nebula at $t > 5 \times 10^5$ yr are insensitive to the uncertainties in the STARBURST 99 model at earlier times. Hence, we can conclude that a nebula older than this age will not be able to explain the observations. The only consistent nebular age estimate derived in § 6.1 is $\sim 2.5 \times 10^4$ yr. The inputs from the STARBURST 99 code are not accurate for such short timescales. Nevertheless, it can be shown that since the ratio between $L_{\rm mech}$ and $N_{\rm Lyc}$ is constant with time, if just the functional dependence of $L_{\rm mech}$ with time for $t < 5 \times 10^5$ yr is reliable, then the model results are rela-

tively independent of the uncertainties in the STARBURST 99 codes. However, given the short ages derived, it can be expected that the star formation at this timescale, and hence the value of L_{mech} and N_{Lyc}, is stochastic, in which case the derived age is inconsistent with the assumptions in the model. Even for a stochastic star formation process, the short dynamical timescale of 10^4 yr needs to be explained. The dynamical model implicitly assumes that the star cluster is spatially within the wind-blown structure, which need not be true for a ≤ 4 pc region. The model also assumes that the stellar wind of the individual stars adds coherently to produce a total '' cluster wind.'' This assumption will be violated for a young cluster because of stellar-wind collisions and young stellar object outflows. These factors may help confine the gas for a longer time and also provide a natural way of increasing the line width by stirring up the intracluster medium. Hence, if a star cluster is invoked as an ionizing source, it must be fairly young, although the properties of such a young cluster cannot be easily predicted.

8.2. *The AGN Model*

We have shown in § 7 that if the proposed AGN hosts a standard thin accretion disk with a BBB, then this disk produces enough UV radiation to ionize the RRL-emitting gas, but its X-ray emission falls short of the observed value. On the other hand, if the AGN has an ADAF disk instead, then again, the observed X-ray emission is insufficient to ionize the RRL-emitting gas. ADAF models also predict the X-ray emission for a given radio flux and mass of the black hole (Yi & Boughn 1998), and the estimated X-ray luminosity is 100 times less than that observed (and is 10 times less than the ratio observed in other LLAGNs; Ulvestad & Ho 2001). A possible way of explaining the observed radio and X-ray fluxes along with the required UV flux is the model of Quataert et al. (1999), who explain the spectrum of two LLAGNs that have an X-ray–to–UV ratio that is too large for a thin disk and too small for an ADAF disk. Following their work, we hypothesize that the possible AGN in the nucleus of NGC 253 has an ADAF disk in the interior, giving way to a standard thin disk beyond a certain radius. In this picture, the radio and the UV emissions arise in the outer disk (which would have a BBB in its spectrum), and the X-ray emission arises from the inner ADAF disk.

8.3. *The Ionizing Source*

It is clear from § 8.1 that if the ionizing source is a star cluster, its age must be at least younger than $\sim 10^5$ yr. The AGN model, discussed in § 8.2, does manage to explain the observations, but the constraints on this model are relatively less in number. The probability of detecting a star cluster of age $\lesssim 10^5$ yr at the radio nucleus would be small. Since there is additional evidence supporting the existence of an AGN at the nucleus, we favor an AGN as the possible ionizing source. The existence of an AGN at the nucleus needs to be confirmed through high-resolution radio continuum or X-ray imaging. The surrounding region has a transitional H II/weak-[O I] low-ionization nuclear emission region (LINER) spectrum (Engelbracht et al. 1998), and hence disentangling the optical signature of an AGN from this LINER emission will be difficult. Detailed multiwavelength modeling of the nuclear emission also needs to be carried out in the framework of the AGN model in order to further constrain the properties of this object.

9. CONCLUSIONS

We have imaged the RRL emission from the starburst galaxy NGC 253 at 8.3 and 15 GHz with a spatial resolution of $\sim 0\rlap{.}''3$ (~ 4 pc) using the VLA. The line emission is maximum at the radio nucleus at both frequencies and is much weaker near the position of the IR peak, which is known to host an SSC. The line widths of both RRLs are large: ~ 200 km s^{-1}. The continuum and line emission were modeled in terms of a uniform-density photoionized gas. The observed RRLs can be explained as arising from a 2–4 pc sized region of gas of mass of a few thousand $M_{\odot}$, at a density of 10^4 cm^{-3}. The ionizing flux required is $(6–20) \times 10^{51}$ photons s^{-1}. This gas can in principle be ionized by a compact SNR, a star cluster, or an AGN. The dust extinction against the nucleus is very high, and hence direct detection of the ionizing source in the optical–IR is not feasible. Detailed dynamical modeling shows that a compact SNR cannot explain the observed properties of the ionized gas. The star cluster model was investigated in terms of a stellar-wind–blown structure. Such a model can only account for all the observed properties for a cluster of age $\sim 2.5 \times 10^4$ yr. Although this age estimate is shown not to be consistent with the dynamical model considered, a relatively young age ($\lesssim 10^5$ yr) for any such cluster is unavoidable. If an AGN is assumed to be the ionizing source, then the observed X-ray flux cannot explain the required ionizing photon rate. However, a simple thin accretion disk model can account for the ionization based on the observed radio flux density. A composite model involving an inner ADAF disk and an outer thin disk is suggested, in order to simultaneously explain the radio, UV, and X-ray observations.

The detection of such a young star cluster at the nucleus of the galaxy is improbable. Since there is additional evidence supporting the existence of an AGN at the nucleus from radio continuum data, we favor the AGN model as an ionizing source. If confirmed, our observations could be the first detection of RRLs from an AGN outside our Galaxy. The central ~ 36 pc region of NGC 253 is host to a number of compact thermal and nonthermal sources and diffuse gas and is also coincident with the base of the galactic superwind and possibly hosts a central AGN as well. Hence, this galaxy would be an ideal laboratory to study the dynamics and the interaction of all these components, much like the Galactic center. Since the submission of this manuscript, K. Weaver et al. (2002, private communication) have found evidence for an obscuring torus and a possible intermediate-mass black hole in the nucleus from hard X-ray data taken with *Chandra*.

REFERENCES

Anantharamaiah, K. R., & Goss, W. M. 1996, ApJ, 466, L13
Anantharamaiah, K. R., Zhao, J.-H., Goss, W. M., & Viallefond, F. 1993, ApJ, 419, 585
Antonucci, R. R. J., & Ulvestad, J. S. 1988, ApJ, 330, L97
Beck, S. C., & Beckwith, S. V. 1984, MNRAS, 207, 671
Böker, T., Krabbe, A., & Storey, J. W. V. 1998, ApJ, 498, L115
Chevalier, R. A., & Fransson, C. 2001, ApJ, 558, L27
Draine, B. T., & Woods, D. T. 1991, ApJ, 383, 621
Engelbracht, C. W., Rieke, M. J., Rieke, G. H., Kelly, D. M., & Achtermann, J. M. 1998, ApJ, 505, 639
Falcke, H., Malkan, M. A., & Biermann, P. L. 1995, A&A, 298, 375
Forbes, D. A., Polehampton, E., Stevens, I. R., Brodie, J. P., & Ward, M. J. 2000, MNRAS, 312, 689
Forbes, D. A., Ward, M. J., & Depoy, D. L. 1991, ApJ, 380, L63
Forbes, D. A., Ward, M. J., Rotaciuc, V., Blietz, M., Genzel, R., Drapatz, S., van der Werf, P. P., & Krabbe, A. 1993, ApJ, 406, L11
Frank, J., King, A. R., & Raine, D. J. 1985, Accretion Power in Astrophysics (Cambridge: Cambridge Univ. Press)
Ho, L. C. 1999, ApJ, 516, 672
Kalas, P., & Wynn-Williams, C. G. 1994, ApJ, 434, 546
Keto, E., Ball, R., Arens, J., Jernigan, G., Meixner, M., Skinner, C., & Graham, J. 1993, ApJ, 413, L23
Keto, E., Hora, J. L., Fazio, G. G., Hoffmann, W., & Deutsch, L. 1999, ApJ, 518, 183
Kobulnicky, H. A., & Johnson, K. E. 1999, ApJ, 527, 154
Koratkar, A., & Blaes, O. 1999, PASP, 111, 1
Leitherer, C., et al. 1999, ApJS, 123, 3
McCray, R. 1983, in Highlights of Astronomy, Vol. 6, ed. R. West (Dordrecht: Reidel), 565
Mebold, U., Shaver, P. A., Bell, M. B., & Seaquist, E. R. 1980, A&A, 82, 272
Meurer, G. R., Heckman, T. M., Leitherer, C., Kinney, A., Robert, C., & Garnett, D. R. 1995, AJ, 110, 2665

Mohan, N. R., Anantharamaiah, K. R., & Goss, W. M. 2001, ApJ, 557, 659
Muñoz-Tuñón, C., Tenorio-Tagle, G., & Castañeda, H. O. 1996, AJ, 112, 1636
Nagar, N. M., Falcke, H., Wilson, A. S., & Ho, L. C. 2000, ApJ, 542, 186
Narayan, R., Mahadevan, R., & Quataert, E. 1998, in Theory of Black Hole Accretion Disks, ed. M. A. Abramowicz et al. (New York: Cambridge Univ. Press), 148
Neff, S. G., & Ulvestad, J. S. 2000, AJ, 120, 670
Newman, W. 1977, Ap&SS, 47, 99
Pietsch, W., et al. 2001, A&A, 365, L174
Piña, R. K., Jones, B., Puetter, R. C., & Stein, W. A. 1992, ApJ, 401, L75
Puxley, P. J., Mountain, C. M., Brand, P. W. J. L., Moore, T. J. T., & Nakai, N. 1997, ApJ, 485, 143
Quataert, E., Di Matteo, T., Narayan, R., & Ho, L. C. 1999, ApJ, 525, L89
Sams, B. J., III, Genzel, R., Eckart, A., Tacconi-Garman, L., & Hofmann, R. 1994, ApJ, 430, L33
Seaquist, E. R., & Bell, M. B. 1977, A&A, 60, L1
Shull, J. M. 1980, ApJ, 238, 860
Spitzer, L. 1968, Diffuse Matter in Space (New York: Interscience)
Tarchi, A., Neininger, N., Greve, A., Klein, U., Garrington, S. T., Muxlow, T. W. B., Pedlar, A., & Glendenning, B. E. 2000, A&A, 358, 95
Turner, J. L., Beck, S. C., & Ho, P. T. P. 2000, ApJ, 532, L109
Turner, J. L., & Ho, P. T. P. 1985, ApJ, 299, L77
Ulvestad, J. S., & Antonucci, R. R. J. 1997, ApJ, 488, 621
Ulvestad, J. S., & Ho, L. C. 2001, ApJ, 562, L133
Vacca, W. D., Garmany, C. D., & Shull, J. M. 1996, ApJ, 460, 914
Watson, A. M., et al. 1996, AJ, 112, 534
Yi, I., & Boughn, S. P. 1998, ApJ, 499, 198
Yorke, H. W., Tenorio-Tagle, G., & Bodenheimer, P. 1984, A&A, 138, 325